Pseudospin-Resolved Transport Spectroscopy of the Kondo Effect in a Double Quantum Dot

S. Amasha,[1] A. J. Keller,[1] I. G. Rau,[2,*] A. Carmi,[3] J. A. Katine,[4] Hadas Shtrikman,[3] Y. Oreg,[3] and D. Goldhaber-Gordon[1,3,†]

[1]*Department of Physics, Stanford University, Stanford, California 94305, USA*
[2]*Department of Applied Physics, Stanford University, Stanford, California 94305, USA*
[3]*Department of Condensed Matter Physics, Weizmann Institute of Science, Rehovot 96100, Israel*
[4]*HGST, San Jose, California 95135, USA*

(Received 6 July 2012; revised manuscript received 13 December 2012; published 24 January 2013)

We report measurements of the Kondo effect in a double quantum dot, where the orbital states act as pseudospin states whose degeneracy contributes to Kondo screening. Standard transport spectroscopy as a function of the bias voltage on both dots shows a zero-bias peak in conductance, analogous to that observed for spin Kondo in single dots. Breaking the orbital degeneracy splits the Kondo resonance in the tunneling density of states above and below the Fermi energy of the leads, with the resonances having different pseudospin character. Using pseudospin-resolved spectroscopy, we demonstrate the pseudospin character by observing a Kondo peak at only one sign of the bias voltage. We show that even when the pseudospin states have very different tunnel rates to the leads, a Kondo temperature can be consistently defined for the double quantum dot system.

DOI: 10.1103/PhysRevLett.110.046604 PACS numbers: 72.15.Qm, 73.21.La, 73.63.Kv

The Kondo effect is one of the paradigms of correlated electron physics [1]. It describes how itinerant electrons with a degenerate degree of freedom screen a localized state with the same degeneracy. Typically, the relevant degeneracy is spin: a localized electron is transitioned between degenerate spin states by spin-flip scattering with conduction electrons. Correlations are established between the localized and conduction electrons, with a many-body spin singlet resulting at low temperatures. This Kondo screening causes a resonance in the local density of states (LDOS) at the Fermi energy, which manifests itself in nanostructures as a zero-bias peak in the conductance [2]. While Kondo physics is usually associated with spin, nanostructures allow the realization of the Kondo effect based on orbital degeneracy [3–7]. The advantage to using an orbital degeneracy is its potential to realize a fully tunable state-resolved probe of Kondo physics that does not perturb the Kondo correlations, which is not possible in spin-based Kondo systems.

Spin-resolved transport measurements in nanostructures have been achieved using ferromagnetic contacts, leading to spin-dependent tunnel rates [8–10]. Unfortunately, these spin-dependent rates also affect Kondo physics [11–14]; moreover, the rates are fixed by the contact design and cannot be tuned. Another approach has been to use a quantum point contact as a spin polarizer [15] to build up a nonequilibrium distribution, with a spin-dependent Fermi energy [16]. However, this technique requires a magnetic field that breaks the spin degeneracy necessary for the Kondo effect.

We instead realize a tunable state-resolved probe of the Kondo effect using an orbital degeneracy of a double quantum dot (DQD) [17,18], which occurs when the energy for an electron to be in dot 1 is the same as that for being in dot 2. These orbital states can be coherently manipulated as a two-level "pseudospin" system [19,20]. The advantage of studying a Kondo effect based on pseudospin degeneracy is that by controlling and measuring each of the dots individually, we can characterize the conductance of each pseudospin component [21–25].

In this Letter, we report pseudospin-resolved transport spectroscopy of the Kondo effect based on an orbital degeneracy in a DQD. We first demonstrate spectroscopy of the DQD analogous to standard transport spectroscopy in a single dot, and we use this to observe the zero-bias peak that is the hallmark of Kondo physics. In standard spectroscopy of spin Kondo, a magnetic field splits the Kondo peak so that the conductance at zero bias is suppressed and the Kondo peaks occur at positive and negative bias. In contrast, pseudospin-resolved spectroscopy of the orbital Kondo effect in a pseudomagnetic field shows a peak at only one sign of the bias, corresponding to the pseudospin state we are observing. Finally, we demonstrate that a single, consistent Kondo temperature can be defined for the entire DQD system.

We measure a laterally gated DQD fabricated from an epitaxially grown AlGaAs/GaAs heterostructure hosting a two-dimensional electron gas with a density of 2×10^{11} cm^{-2} and a mobility of 2×10^{6} cm^2/V s. We apply negative voltages to metallic surface gates (inset of Fig. 1) to form two capacitively coupled quantum dots with negligible interdot tunneling [26]. The gates W1L and W1U control the tunneling rates between dot 1 and its source and drain leads $\Gamma_{S1}/\hbar$ and $\Gamma_{D1}/\hbar$, respectively. We define $\Gamma_1 = \Gamma_{S1} + \Gamma_{D1}$, and Γ_2 analogously for dot 2. The conductances of the dots are measured using separate circuits. All the

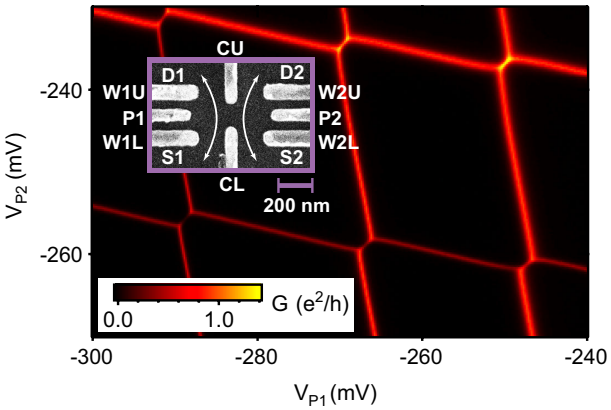

FIG. 1 (color online). The sum of measured zero-bias conductances through dots 1 and 2 ($G = G_1 + G_2$) as a function of the voltages on the gates labeled $P1$ and $P2$ (V_{P1} and V_{P2}, respectively). Inset: A scanning electron micrograph of a device similar to the one measured. The gates that define the DQD as well as the source and drain leads for dot 1 ($S1$ and $D1$) and for dot 2 ($S2$ and $D2$) are labeled. Arrows have been drawn to emphasize the paths through which currents are measured.

data in this Letter are taken with $B \leq 80$ mT, so that spin degeneracy is maintained.

Figure 1 shows the results of summing the zero-bias conductance measured through dots 1 and 2 (denoted G_1 and G_2, respectively) as a function of the voltages applied to the gates $P1$ and $P2$, which control the occupancy of the dots. The Coulomb blockade lines delineate the "honeycomb" shape of the DQD charge stability diagram [27]. From these data we extract intradot charging energies of $U_1 \approx 1.2$ meV and $U_2 \approx 1.5$ meV, as well as an interdot charging energy $U' \approx 100$ μeV.

For the data in Fig. 1, Γ_1 and Γ_2 are between 20 and 50 μeV. Since $\Gamma_1 \ll U_1$ and $\Gamma_2 \ll U_2$, the spin Kondo temperature is much less than the electron temperature of 22 mK and we do not observe Kondo-enhanced conductance due to spin degeneracy in the odd Coulomb valleys. However, in this regime $\Gamma_{1,2}/U' \sim 0.2$–0.5 and between each pair of triple points visible in the figure we observe Kondo-enhanced conductance where there is an orbital degeneracy [17]. In contrast to Ref. [18], we observe enhancements at all orbital degeneracies, regardless of whether the dots contain an even or odd number of electrons. As spin degeneracy has not been broken, it should play a role [28], but many of the salient features can be explained by considering the orbital degeneracy.

To perform the analogue of standard bias spectroscopy on a DQD, we apply an equal voltage to both the pseudospin-up source ($S1$) and the pseudospin-down source ($S2$), while varying the energy of the orbital states E and maintaining their degeneracy ($\delta = 0$); see Fig. 2(a). We accomplish this by determining the capacitance factors that relate changes in V_{P1}, V_{P2}, V_{S1}, and V_{S2} to changes in the energies of the dots [26]. This allows us to find the gate voltages necessary to effect a change in either the average

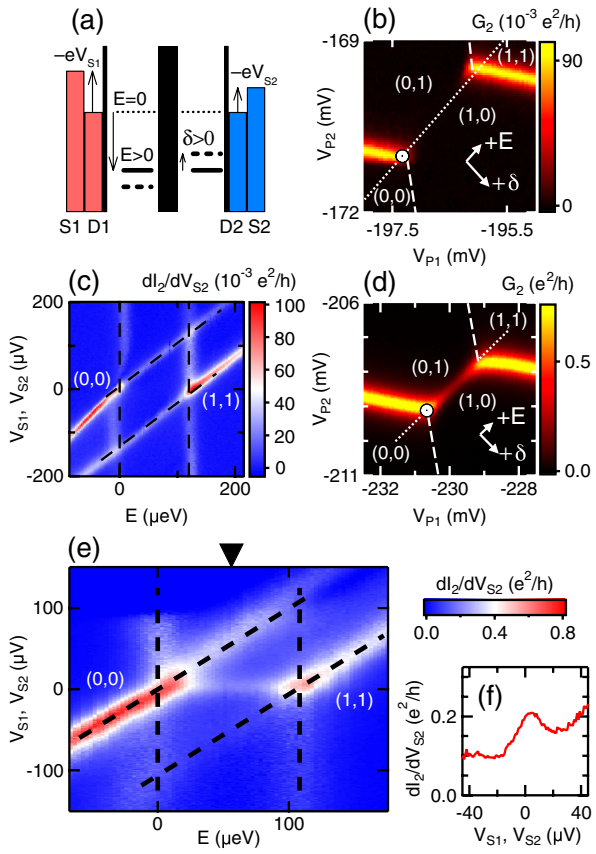

FIG. 2 (color online). (a) DQD energy diagram showing (from left to right) dot 1's leads, confinement potential, and chemical potential (solid horizontal line). A thick tunnel barrier emphasizes the negligible interdot tunneling, and then there is an analogous picture for dot 2. Leads $S1$ and $S2$ may be independently biased by voltages V_{S1} and V_{S2}. E is the energy of the dot states below the Fermi energy of the drains, while δ is the energy difference between the dot states (the solid lines show the levels at $\delta = 0$ while the dashed lines show how the levels shift with positive δ). (b) G_2 for $\Gamma_{1,2}/U \approx 0.13$ showing the dot 2 Coulomb blockade peaks. The dashed lines show where the dot 1 peaks are observed in measurements of G_1. The ordered pairs list the occupation of the dot states relative to some background occupation. The vectors along which V_{P1} and V_{P2} are simultaneously swept in order to change E or δ by $+25$ μeV are shown. The dotted line corresponds to the horizontal axis in (c) at zero bias and the white dot marks $E = 0$ and $\delta = 0$ at zero bias. (c) Bias spectroscopy of dot 2 at $\delta = 0$, when the pseudospin states are degenerate. (d) G_2 in the double dot Kondo regime with $\Gamma_{1,2}/U \approx 0.24$. The dotted line corresponds to the horizontal axis in (e) at zero bias. (e) Bias spectroscopy for dot 2 at $\delta = 0$ in the Kondo regime. The black arrow shows the location of the cut shown in (f).

energy E or the detuning δ of the double dot system [vectors in Fig. 2(b)] for given bias voltages.

In the Coulomb blockade regime, standard spectroscopy of the DQD shows the characteristic diamond-shaped regions of suppressed conductance. Figure 2(b) shows the conductance through dot 2 when $\Gamma_{1,2}/U' \ll 1$ and Kondo screening is suppressed, while the corresponding

spectroscopy measurements are shown in Fig. 2(c). The slopes of the Coulomb diamond edges are as predicted: the vertical dashed lines correspond to alignment of the dot levels with their drain leads while the dashed lines with slope 1 correspond to alignment with the source leads [26]. This agreement demonstrates the high fidelity of our control over E and δ.

As Γ_1 and Γ_2 are increased, we observe a conductance enhancement along a line between a pair of triple points, where two orbital states are degenerate [Fig. 2(d)]. The corresponding spectroscopy data are shown in Fig. 2(e) and exhibit a zero-bias peak in the middle of the Coulomb diamond. This provides clear evidence that the conductance enhancement results from Kondo screening.

To demonstrate pseudospin-resolved spectroscopy, as well as the importance of orbital degeneracy, we can break this degeneracy. We can gain intuition about the results by considering the spin Kondo effect in a single dot in a magnetic field. Above a threshold field, the peak in the LDOS splits above and below the Fermi energy of the leads by the Zeeman energy E_Z [29,30]. The lower energy peak is associated with spin-up and the higher energy peak with spin-down [Fig. 3(a)]. At zero bias, the peaks are no longer aligned with the Fermi energy and no conductance enhancement is observed. The spin-dependent nature of the peaks can be resolved by independently varying the electrochemical potential of one spin species. For example, if the spin-up electrons are biased so that their electrochemical potential aligns with the spin-up peak ($V_{S,\uparrow} = +E_Z/e$), then the conductance enhancement should be observed [Fig. 3(b)]. Specifically, a spin-down electron can tunnel on from either lead, temporarily violating energy conservation. The spin-up electron can then tunnel out to the source lead, restoring energy conservation and flipping the spin of the dot. This and higher-order spin-flip processes constitute the nonequilibrium Kondo effect. Similar spin-flip processes occur if the spin-down electrons are biased to align with the spin-down peak. In contrast, when the spin-up electrons are biased to align with the spin-down peak

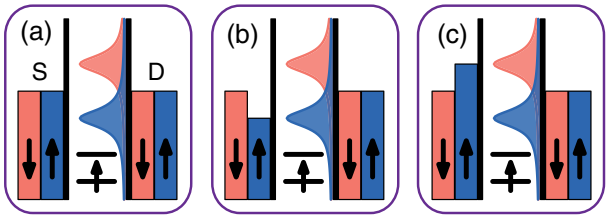

FIG. 3 (color online). (a) Spin-1/2 Kondo effect for a single dot in a magnetic field. The diagram depicts a spin-resolved source lead, a spin-split Kondo peak in the LDOS (for clarity, we show the peaks associated only with the drain lead), and a spin-resolved drain lead. At zero bias, no Kondo enhancement is observed. (b) When the spin-up source lead is biased by $V_{S,\uparrow} = +E_Z/e$, Kondo-enhanced conductance is observed. (c) For $V_{S,\uparrow} = -E_Z/e$, no Kondo enhancement occurs.

($V_{S,\uparrow} = -E_Z/e$), these spin-flip processes are not possible and no enhancement should be observed [Fig. 3(c)].

Standard bias spectroscopy of spin Kondo in a single dot in a magnetic field does not resolve the spin-dependent nature of the resonances: the bias changes the electrochemical potential of both spin species so the Kondo enhancement appears at both signs of the bias voltage $V_S = \pm E_Z/e$ [31,32]. However, in a DQD one can perform the pseudospin-resolved measurement by varying the bias on only $S1$, corresponding to changing the electrochemical potential of the pseudospin-up electrons. To realize this pseudospin-resolved spectroscopy we apply a finite detuning to establish a pseudo-Zeeman splitting $E_{pZ} = 2\delta$ [dashed gray (blue in online figure) line in Fig. 4(a), along which $E_{pZ} = -20$ μeV]. The corresponding pseudospin-resolved bias spectroscopy data are shown for dot 1 in Fig. 4(b). There is no longer an enhancement at zero bias; rather, we observe the Kondo peak at a finite bias voltage. The peak location is in good agreement with the expected value, $V_{S1} = E_{pZ}/e = -20$ μV, indicated by the gray arrow along the vertical axis. Most importantly, there is no Kondo enhancement at positive bias, demonstrating pseudospin resolution in measurement of the Kondo-enhanced density of states.

As Kondo screening involves pseudospin flips, at $V_{S1} = E_{pZ}/e$ we also expect to see an enhancement in the conductance through dot 2. This is validated in Fig. 4(c), where we show spectroscopy of dot 2 as a function of V_{S1}. Figure 4(d) shows cuts through the data in Figs. 4(b) and 4(c) indicated by the black arrows. As expected, peak conduction occurs at the same V_{S1} value for both dots. The V_{S1} position of the resonance depends on E_{pZ} as predicted [Figs. 4(e) and 4(f)]: the extracted positions are shown in the inset of Fig. 4(e), and the agreement with the solid line demonstrates $V_{S1} = E_{pZ}/e$ up to a small offset. Pseudospin spectroscopy as a function of V_{S2} [Figs. 4(g) and 4(h)] shows the behavior of the pseudospin-down peak, which has a negative slope as a function of E_{pZ}. For the data in Fig. 4 (which are taken with different gate voltage settings than in Fig. 2), we estimate $\Gamma_{D1}/\Gamma_{S1} \approx 0.09$ and $\Gamma_{D2}/\Gamma_{S2} \approx 0.3$ [26]. These settings allow observation of the feature at $E_{pZ} = 0$ in Fig. 4(g) (see Ref. [26]).

The data in Fig. 4(d) show that the widths of the peaks in dots 1 and 2 are equal, indicating that we can define a consistent T_K for the DQD. We check that we can continue to define a consistent T_K when the pseudospin components have very different couplings to their leads (e.g., $\Gamma_1 < \Gamma_2$), so that the tunneling rates are pseudospin dependent. This is analogous to contacting a nanostructure with ferromagnetic leads, although the DQD offers the advantage of probing each pseudospin component independently. Figure 5 shows data taken when $\Gamma_2/\Gamma_1 \approx 2.4$, and the Kondo enhancement is still observed. Cuts through the data are shown in Fig. 5(c) and show good agreement between the peak widths. The temperature dependence of

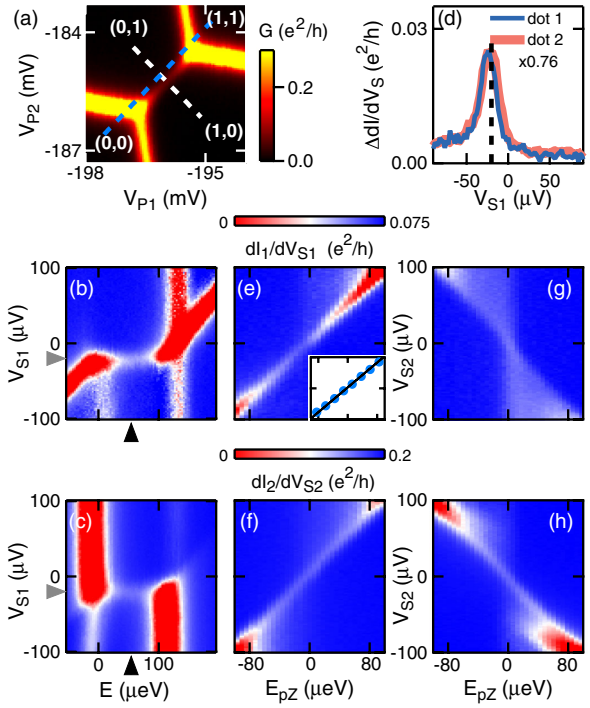

FIG. 4 (color online). (a) $G = G_1 + G_2$ as a function of V_{P1} and V_{P2}. Along the dashed gray (blue in online figure) line E changes while $E_{pZ} = -20$ μeV. Along the dashed white line E_{pZ} varies while E is constant. (b) Pseudospin-resolved bias spectroscopy for dot 1. The horizontal axis at zero bias corresponds to the dashed gray (blue in online figure) line in (a). The gray arrow on the vertical axis marks $V_{S1} = E_{pZ}/e = -20$ μV. The color scale above (e) applies to (b), (e), and (g). (c) Pseudospin-resolved bias spectroscopy for dot 2 as a function of V_{S1}. The color scale above (f) applies to (c), (f), and (h). (d) Cuts through the data [black arrows in (b) and (c)] explicitly showing the Kondo enhancement. The dashed black line indicates $V_{S1} = -20$ μV. The dot 2 data are scaled by 0.76 and a conductance offset is subtracted to allow comparison of the Kondo peak widths. (e) Pseudospin-resolved spectroscopy through dot 1 as E_{pZ} is varied [horizontal axis at zero bias corresponds to dashed white line in (a)]. The inset shows the position of the peak in V_{S1} (vertical axis, limits are ± 100 μV) as a function of E_{pZ} (horizontal axis, limits are ± 100 μeV). The solid black line shows the result of fitting to $V_{S1} = E_{pZ}/e + c$ with the offset c as the only fit parameter. (f) Pseudospin-resolved spectroscopy through dot 2 as a function of V_{S1}. Since Kondo involves pseudospin flips, the Kondo enhancement observed in dot 1 in (e) gives a corresponding enhancement in dot 2. Pseudospin-resolved spectroscopy as a function of V_{S2} is shown for dot 1 (g) and dot 2 (h).

the width shown in Fig. 5(d) demonstrates that this agreement is maintained over the entire temperature range measured. These data confirm that a single consistent T_K scale can be defined across both pseudospin components, even with very asymmetric coupling.

In conclusion, we report pseudospin-resolved spectroscopy of a DQD. In a pseudomagnetic field, we observe Kondo-enhanced conductance at opposite biases for the

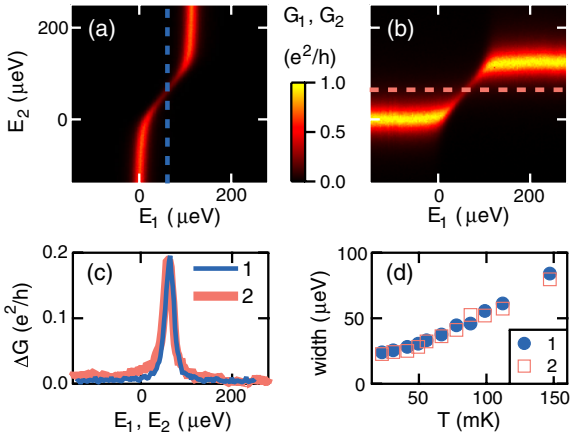

FIG. 5 (color online). (a), (b) Zero-bias conductance of dot 1 (a) and dot 2 (b) for $\Gamma_1 = 19$ μeV and $\Gamma_2 = 45$ μeV. The axes refer to the energy of the dot 1 ($E_1 = E + \delta$) and dot 2 ($E_2 = E - \delta$) states relative to the drain leads. (c) Conductance cuts through the data indicated by the dashed lines in (a) and (b). To compare the Kondo peak widths a constant conductance background was subtracted from the dot 2 data, but no vertical scaling was necessary. (d) Full width at half maximum measured from cuts like those in (c) as a function of temperature.

two pseudospins, revealing the pseudospin dependence of the split Kondo resonance. We also demonstrate that T_K is well defined in the pseudospin system. These measurements demonstrate the unique capabilities of DQDs to probe the many-body Kondo state.

We are grateful to G. Zaránd, C. P. Moca, I. Weymann, S. E. Ulloa, G. B. Martins, C. A. Büsser, A. E. Feiguin, and M. R. Calvo for discussions. This work was supported by the NSF under Contract No. DMR-0906062 and by the U.S.-Israel BSF Grant No. 2008149. A. J. K. acknowledges a Stanford Graduate Fellowship and D. G.-G. acknowledges the Weston Visiting Professorship at the Weizmann Institute.

*Present address: IBM Almaden Research Center, San Jose, California 95120, USA.

†Present address: Stanford University, Stanford, California 94305, USA.
goldhaber-gordon@stanford.edu

[1] A. C. Hewson, *The Kondo Problem to Heavy Fermions*, Cambridge Studies in Magnetism (Cambridge University Press, Cambridge, England, 1993).

[2] M. Grobis, I. G. Rau, R. M. Potok, and D. Goldhaber-Gordon, in *Handbook of Magnetism and Advanced Magnetic Materials* (John Wiley and Sons, Chichester, England, 2007), Vol. 5.

[3] U. Wilhelm, J. Schmid, J. Weis, and K. von Klitzing, Physica (Amsterdam) **14E**, 385 (2002).

[4] A. W. Holleitner, A. Chudnovskiy, D. Pfannkuche, K. Eberl, and R. H. Blick, Phys. Rev. B **70**, 075204 (2004).

[5] P. Jarillo-Herrero, J. Kong, H. S. J. van der Zant, C. Dekker, L. P. Kouwenhoven, and S. D. Franchesi, Nature (London) **434**, 484 (2005).
[6] D. M. Schröer, A. K. Hüttel, K. Eberl, S. Ludwig, M. N. Kiselev, and B. L. Altshuler, Phys. Rev. B **74**, 233301 (2006).
[7] A. Makarovski, J. Liu, and G. Finkelstein, Phys. Rev. Lett. **99**, 066801 (2007).
[8] A. N. Pasupathy, R. C. Bialczak, J. Martinek, J. E. Grose, L. A. K. Donev, P. L. McEuen, and D. C. Ralph, Science **306**, 86 (2004).
[9] J. R. Hauptmann, J. Paaske, and P. E. Lindelof, Nat. Phys. **4**, 373 (2008).
[10] M. R. Calvo, J. Fernandez-Rossier, J. J. Palacios, D. Jacob, D. Natelson, and C. Untiedt, Nature (London) **458**, 1150 (2009).
[11] J. Martinek, Y. Utsumi, H. Imamura, J. Barnaś, S. Maekawa, J. König, and G. Schön, Phys. Rev. Lett. **91**, 127203 (2003).
[12] J. Martinek, M. Sindel, L. Borda, J. Barnaś, J. König, G. Schön, and J. von Delft, Phys. Rev. Lett. **91**, 247202 (2003).
[13] R. López and D. Sánchez, Phys. Rev. Lett. **90**, 116602 (2003).
[14] M. Sindel, L. Borda, J. Martinek, R. Bulla, J. König, G. Schön, S. Maekawa, and J. von Delft, Phys. Rev. B **76**, 045321 (2007).
[15] R. M. Potok, J. A. Folk, C. M. Marcus, V. Umansky, M. Hanson, and A. C. Gossard, Phys. Rev. Lett. **91**, 016802 (2003).
[16] T. Kobayashi, S. Tsuruta, S. Sasaki, T. Fujisawa, Y. Tokura, and T. Akazaki, Phys. Rev. Lett. **104**, 036804 (2010).
[17] A. Hübel, K. Held, J. Weis, and K. v. Klitzing, Phys. Rev. Lett. **101**, 186804 (2008).
[18] Y. Okazaki, S. Sasaki, and K. Muraki, Phys. Rev. B **84**, 161305 (2011).
[19] T. Fujisawa, T. Hayashi, H. Cheong, Y. Jeong, and Y. Hirayama, Physica (Amsterdam) **21E**, 1046 (2004).
[20] K. D. Petersson, J. R. Petta, H. Lu, and A. C. Gossard, Phys. Rev. Lett. **105**, 246804 (2010).
[21] L. Borda, G. Zaránd, W. Hofstetter, B. I. Halperin, and J. von Delft, Phys. Rev. Lett. **90**, 026602 (2003).
[22] D. Feinberg and P. Simon, Appl. Phys. Lett. **85**, 1846 (2004).
[23] R. López, D. Sánchez, M. Lee, M.-S. Choi, P. Simon, and K. Le Hur, Phys. Rev. B **71**, 115312 (2005).
[24] A. Carmi, Y. Oreg, and M. Berkooz, Phys. Rev. Lett. **106**, 106401 (2011).
[25] C. A. Büsser, A. E. Feiguin, and G. B. Martins, Phys. Rev. B **85**, 241310(R) (2012).
[26] See Supplemental Material at http://link.aps.org/supplemental/10.1103/PhysRevLett.110.046604 for additional details about bias spectroscopy and the interdot and dot-lead couplings.
[27] W. G. van der Wiel, S. De Franceschi, J. M. Elzerman, T. Fujisawa, S. Tarucha, and L. P. Kouwenhoven, Rev. Mod. Phys. **75**, 1 (2002).
[28] A. J. Keller (to be published).
[29] Y. Meir, N. S. Wingreen, and P. A. Lee, Phys. Rev. Lett. **70**, 2601 (1993).
[30] T. A. Costi, Phys. Rev. Lett. **85**, 1504 (2000).
[31] D. Goldhaber-Gordon, H. Shtrikman, D. Mahalu, D. Abush-Magder, U. Meirav, and M. A. Kastner, Nature (London) **391**, 156 (1998).
[32] A. Kogan, S. Amasha, D. Goldhaber-Gordon, G. Granger, M. A. Kastner, and H. Shtrikman, Phys. Rev. Lett. **93**, 166602 (2004).